



# A study of structural differences between liver cancer cells and normal liver cells using FTIR spectroscopy



Daping Sheng<sup>a, b, 1</sup>, Fangcheng Xu<sup>b, 1</sup>, Qiang Yu<sup>a</sup>, Tingting Fang<sup>a, c</sup>, Junjun Xia<sup>a, c</sup>, Seruo Li<sup>a, c</sup>, Xin Wang<sup>a, \*</sup>

<sup>a</sup> School of Basic Medical Sciences, Anhui Medical University, Hefei, Anhui 230032, China

<sup>b</sup> The First Affiliated Hospital, Anhui Medical University, Hefei, Anhui 230032, China

<sup>c</sup> The First Clinical College, Anhui Medical University, Hefei, Anhui 230032, China

## ARTICLE INFO

### Article history:

Received 14 December 2014

Received in revised form

20 May 2015

Accepted 22 May 2015

Available online 17 June 2015

### Keywords:

FTIR spectroscopy

IR spectra

Liver cancer

Cell

## ABSTRACT

Since liver cancer seriously threatens human health, it is very urgent to explore an effective method for diagnosing liver cancer early. In this study, we investigated the structure differences of IR spectra between neoplastic liver cells and normal liver cells. The major differences of absorption bands were observed between liver cancer cells and normal liver cells, the values of A2955/A2921, A1744/A1082, A1640/A1535, H1121/H1020 might be potentially useful factors for distinguishing liver cancer cells from normal liver cells. Curve fitting also provided some important information on structural differences between malignant and normal liver cancer cells. Furthermore, IR spectra combined with hierarchical cluster analysis could make a distinction between liver cancer cells and normal liver cells. The present results provided enough cell basis for diagnosis of liver cancer by FTIR spectroscopy, suggesting FTIR spectroscopy may be a potentially useful tool for liver cancer diagnosis.

© 2015 Elsevier B.V. All rights reserved.

## 1. Introduction

As one of the most common malignancies worldwide, liver cancer ranks third in cancer-related death [1]. According to the statistics of World Health Organization (WHO) in 2008, 748,300 new liver cancer cases were diagnosed while 695,900 cases died annually in the world, and more than 50% of them occurred in China [2]. The primary cause of liver cancer includes infection of viral hepatitis, aflatoxin contamination of food, pollution of drinking water and some other factors [3]. Now resection or liver transplantation is very effective for treating liver cancer, but unfortunately, most liver cancer patients are diagnosed at the middle or late stage which leads to the loss of the best time for treatment, so the 5-year survival rate of liver cancer patients is only 3%–5% [4]. Therefore, it is very important to detect liver cancer at the early stage. At present, serum alpha-fetoprotein (AFP) has been widely used for liver cancer diagnosis, but AFP concentration in most of hepatocellular carcinoma patients did not elevate at the early stage

while AFP concentration was found to increase in some chronic hepatitis or cirrhotic patients [4,5]. Imaging examination is also often used for liver cancer screening, but it has several disadvantages such as difficulty in distinguishing liver cancer from non-malignant hyperplasia, the high cost for some images (CT, MRI, etc.) and the dependence on operators' experience [3]. Now many methods have been developed to study the pathogenesis, diagnosis and treatment of liver cancer.

Since FTIR spectroscopy can investigate biochemical changes of cells/tissues effectively and non-invasively at molecular level [6], it has been widely used to investigate colorectal cancer [7,8], gastric cancer [9], prostate cancer [10], papillary thyroid carcinoma [11], breast cancer [12], ovarian cancer [13,14], urinary bladder cancer [15] and other cancers [16–22]. There were also some reports on FTIR spectroscopic study of liver diseases such as liver cancer [5,23,24] and hepatic fibrosis [25,26], for example, Zhang et al. differentiated cirrhotic patients with hepatocellular carcinoma (HCC) from cirrhotic patients without HCC using FTIR spectroscopy [5], Feng et al. used FTIR spectroscopy to investigate the effects of several traditional Chinese medicines on liver cancer cell line SMMC-7221 [24], Scaglia et al. reported the potential use of sera's FTIR spectra for distinguishing chronic hepatitis C (CHC) patients with hepatic fibrosis from CHC patients without hepatic

Abbreviations: FTIR, Fourier transform infrared; IR, Infrared.

\* Corresponding author.

E-mail address: [wxchem81@tom.com](mailto:wxchem81@tom.com) (X. Wang).

<sup>1</sup> Both contributed equally to this work.

fibrosis [26]. However, to our knowledge, the number of these reports was few. In this study, biochemical changes of liver cancer cells compared to normal liver cells were investigated by FTIR spectroscopy at the molecular level. The goal of our study was to provide some helpful information for gaining insight into the pathogenesis of liver cancer, moreover, give cell basis for diagnosing liver cancer with FTIR spectroscopy.

## 2. Materials and methods

### 2.1. Cell culture

Three human liver cancer cell lines: SMMC-7721 (poorly differentiated), Bel-7402 (moderately differentiated) and HepG2 (well differentiated) and a normal human liver cell line LO2 were used in this study. The cells were cultured in DMEM medium containing 10% fetal bovine serum (heat-inactivated), 100 unit/ml penicillin and 100  $\mu$ g/ml streptomycin. Moreover, the cells were incubated at 37°C in a 5% CO<sub>2</sub> humidified atmosphere for 24 h.

### 2.2. Sample preparation

After culture, the cells were collected by centrifugation, washed with 0.9% NaCl solution for 3 times and then re-suspended in 0.9% NaCl solution. About 5  $\mu$ l cell suspension was deposited on an IR-transparent BaF<sub>2</sub> window and then dried under vacuum at room temperature.

### 2.3. FTIR spectroscopic examination

All spectra were recorded with an FTIR spectrometer (IRAffinity-1, SHIMADZU Corporation) equipped with a DLATGS detector. For each spectrum, 64 scans were co-added with a 4 cm<sup>-1</sup> resolution in the region of 4000–800 cm<sup>-1</sup>. IRsolution software was used to collect spectral data and store these data as JCAMP format.

### 2.4. Data procession

The spectral data (JCAMP format) were processed by OPUS5.5 software subsequently. All spectra were baseline corrected and then min–max normalized to the amide I band in the 1750–800 cm<sup>-1</sup> region. In the higher wavenumber region, the spectra were cut between 3650 and 2800 cm<sup>-1</sup>, baseline corrected and then min–max normalized to the amide A band. Curve fitting was performed in the regions of 1564–1480 cm<sup>-1</sup> and 1326–1182 cm<sup>-1</sup> respectively by origin 6.0 software (Gaussian formula), the curves for curve fitting were obtained from the secondary derivative IR spectra (Savitzky-Golay algorithm and nine smoothing points). Hierarchical cluster analysis was done by SPSS19.0 software.

## 3. Results

### 3.1. Analysis of IR spectra

The spectra of liver cancer cells and normal liver cells were displayed in Fig. 1. The peak positions and their assignments were listed in Table 1 [27–34]. Since the spectral resolution was 4 cm<sup>-1</sup>, the peak shifts below 4 cm<sup>-1</sup> could not be distinguished. The structural differences were summarized as follows:

**Amide Bands** The amide A band peaked at around 3282 cm<sup>-1</sup> for cancer cells, whereas this peak was shifted to 3317 cm<sup>-1</sup> for normal cells, which might result from the changes of the hydrogen-bonded N–H groups in proteins. The amide I band was located around 1644 cm<sup>-1</sup> for cancer cells while it was located at 1630 cm<sup>-1</sup> for normal cells, which might be connected with the changes of the

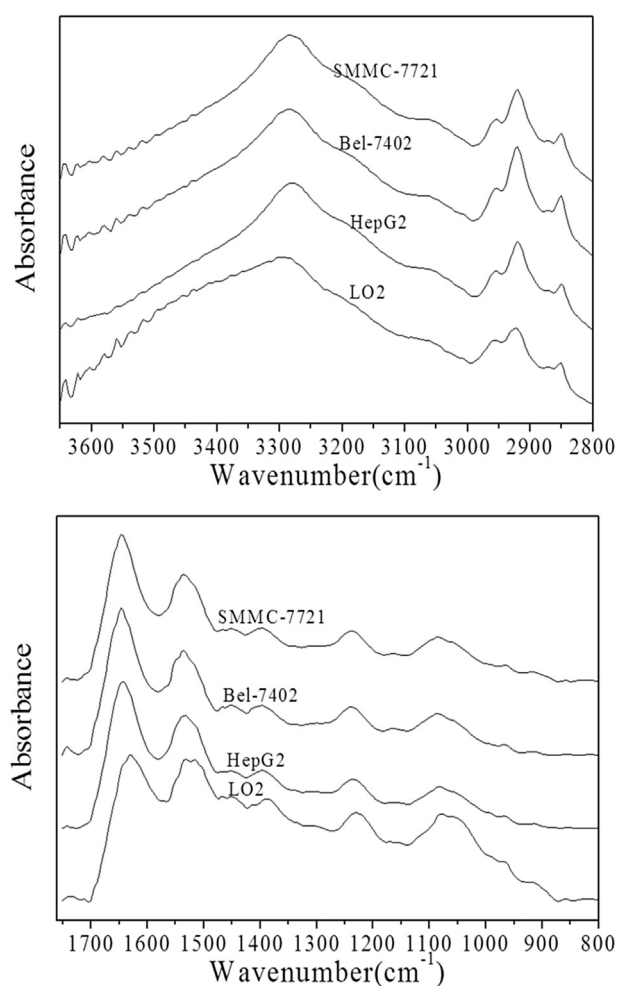


Fig. 1. IR spectra of liver cancer cell lines and normal liver cell line.

**Table 1**  
Preliminary assignments of liver cells' IR spectra.

Frequency (cm <sup>-1</sup> )				Assignments
SMMC-7721	Bel-7402	HepG2	LO2	
3283	3284	3281	3317	the amide A band
2955	2955	2955	2956	asymmetric C–H stretching of CH <sub>3</sub>
2921	2921	2920	2923	asymmetric C–H stretching of CH <sub>2</sub>
2872	2872	2873	2872	symmetric C–H stretching of CH <sub>3</sub>
2851	2852	2851	2852	symmetric C–H stretching of CH <sub>2</sub>
1744	1744	1744	1740	C=O stretching
1646	1646	1644	1630	the amide I band
1535	1536	1533	1532	the amide II band
1452	1453	1452	1453	CH <sub>2</sub> deformation
1396	1396	1396	1391	CH <sub>3</sub> bending/C=O stretching
1300	1300	1311	1312	the amide III band
1239	1239	1238	1230	asymmetric stretching of PO <sub>2</sub> <sup>-</sup>
1168	1164	1168	1170	C–O (H) stretching
1084	1085	1083	1079	symmetric stretching of PO <sub>2</sub> <sup>-</sup>
967	967	967	971	C–C/C–O stretching
916	916	916	919	D-glucopyranose ring vibrations
860	857	855	857	α-1,6-glucans

secondary protein structures. Simultaneously, the obvious differences also existed in other protein bands. The amide II band in Bel-7402 peaked at 1536 cm<sup>-1</sup> while it was shifted to 1532 cm<sup>-1</sup> in LO2. The amide III band was located at 1300 cm<sup>-1</sup> for SMMC-7721 and Bel-7402 while it was located at around 1311 cm<sup>-1</sup> for HepG2 and

Download English Version:

<https://daneshyari.com/en/article/1401730>

Download Persian Version:

<https://daneshyari.com/article/1401730>

[Daneshyari.com](https://daneshyari.com)